



Cloud characteristics in the Aravalli ranges of Western India: Insights from ground-based Lidar measurements

Dharmendra Kumar Kamat^{1,2} · Som Kumar Sharma¹ · Kondapalli Niranjan Kumar³ · Prashant Kumar⁴ · Sourita Saha⁵

Received: 8 June 2024 / Accepted: 5 August 2024

© The Author(s), under exclusive licence to Springer Nature Switzerland AG 2024

Abstract

Clouds are integral components of the hydrological cycle and exert significant influence on regional and global weather patterns. Understanding cloud height, layers, and fraction in the atmosphere is crucial for precipitation and regulating Earth's energy balance. This study investigates the cloud characteristics such as the cloud base height (CBH), cloud top height (CTH), and the vertical visibility over Udaipur, an urban city situated in the Aravalli ranges of Western India, employing ground-based Lidar (Ceilometer), satellite (MODIS), and reanalysis datasets (ERA5). The analysis focuses on CBH observations from Ceilometer Lidar during 2021-22, evaluating reanalysis and satellite-derived CBH. Results reveal peak detection (cloud presence or fully obscured sky) during the southwest monsoon, with frequencies reaching approximately 44%, 79%, 71%, and 37% in June, July, August, and September, respectively. While single-layer clouds are prevalent throughout the observation period, multiple layers are primarily observed during the monsoon, peaking in July and August. CBH exhibits a seasonal pattern, remaining low during the monsoon and high during pre-monsoon periods. Cloud type quantification based on CTH properties from MODIS satellites shows cirrostratus clouds as the most prevalent (approximately 36%) during the study period. Although CBH derived from MODIS CTH aligns with Ceilometer observations, the overall correlation is weak. Additionally, a seasonal variation is observed in ERA5 reanalysis performance regarding cloud base height detection over Udaipur. Therefore, the findings could contribute to broader scientific knowledge on cloud formation over complex hilly regions and these insights are crucial for improving weather prediction models by offering detailed data on cloud behavior, essential for accurate local weather forecasts.

Keywords Cloud base height · Lidar · Ceilometer · MODIS · ERA5 reanalysis

1 Introduction

Clouds cover most of the Earth (~67%), and even a slight variation in their properties can disturb the radiation budget, modulate weather, and impact climate change (King et al. 2013; Ramanathan et al. 1989; Stubenrauch et al. 2013). Due to their crucial roles in the climate system, including the radiative budget, hydrological cycle, and various cloud feedback processes, the study of clouds has remained pivotal in climate research. The radiative effect of clouds depends on factors such as cloud height, amount, thickness, phase, and microphysical properties (Schmetz 2016; Stephens and Webster 1981). Given their dynamic nature in space and time, accurately representing clouds in weather and climate models poses significant challenges. Improper representation of these parameters introduces uncertainty in models, making it difficult to accurately predict future weather and climate. Therefore, continuous monitoring and investigation of clouds is essential for climate diagnosis and forecasting.

Cloud properties such as cloud base height (CBH), cloud top height (CTH), cloud fraction, and vertical layer structure significantly affect the radiative balance, atmospheric circulations, and other meteorological processes (Lü et al. 2015; Samanta et al. 2020). The lack of comprehensive observations and an incomplete understanding of various cloud processes have made cloud representation in weather and climate models a dominant source of uncertainty for decades (Bony et al. 2006; Cess et al. 1989; Randall et al. 2003). Remote sensing techniques, both ground-based and satellite-based, are commonly used to study cloud properties. While passive remote sensing from satellites typically provides detailed observations of high-level clouds, it often struggles with accurately detecting low and mid-level clouds. Nonetheless, satellite observations are invaluable for retrieving global information related to CTH. However, there is a need to further enhance the accuracy in measuring CTH and deriving CBH using the cloud properties (An et al., 2019).

Satellite observations alone have limitations in accurately detecting cloud base properties like CBH. Integrating ground-based observations with satellite data can help bridge these gaps and improve our understanding of clouds effects on climate, such as cloud radiative forcing (Xu et al. 2021). Ground-based detection of clouds is gaining importance due to its reliability and high temporal and vertical resolution. Lidar, a powerful instrument for investigating cloud characteristics and vertical structure from the ground, has become increasingly prevalent with advancements in laser technology (Wang and Menenti 2021). The Ceilometer, a low power Lidar, is widely used for continuous ground-based measurement of CBH due to its high temporal and vertical resolution (Costa-Surós et al. 2013).

Several studies have utilized Ceilometers to examine cloud base and vertical structure across different parts of the world (Lee et al. 2018; Martucci et al. 2010; Maturilli and Ebell 2018; Sharma et al. 2016; Viúdez-Mora et al. 2015). For instance, Martucci et al. (2010) retrieved the multilayer cloud base heights using two different collocated Ceilometers at the Mace Head Atmospheric Research Station in Ireland. The study reported significant differences in the CBH outputs from the two Ceilometers. Viúdez-Mora et al. (2015) used a Ceilometer to observe CBH and study overcast conditions at Girona (NE Iberian Peninsula) based on a radiative transfer model, finding good correlation between calculated cloud radiative effect values and observations. The study showed that the calculated cloud radiative effect values correlate well with the observations when the Ceilometer observed CBH is used in the model. Maturilli and Ebell (2018) studied the annual cycle of cloud occurrence

frequency over Ny-Ålesund, Svalbard, and the Arctic using 25 years of CBH observations from Ceilometers. Lee et al. (2018) investigated the relationship between CBH, cloud frequency, and precipitation over two urban locations in Seoul, Korea, using a Ceilometer and microwave radiometer. Sharma et al. (2016) compared CBH observed from a Ceilometer to that derived from the Moderate Resolution Imaging Spectroradiometer (MODIS) on board Aqua and Terra satellites over the Ahmedabad region. Another study by Vaishnav et al. (2019) performed a statistical analysis of CBH and the seasonal variation of cloud occurrence frequency over the same region. These ground-based observations are crucial for enhancing regional and global weather and climate models, providing better quality ground truth data for model inputs.

The vertical distribution of clouds, including their height, layering, and thickness, plays a pivotal role in the Earth's radiation budget. However, accurately representing this distribution remains a significant challenge in both regional and global climate models, leading to uncertainties in climate projections. Previous research has highlighted the influence of cloud vertical structure on atmospheric circulation and precipitation (Kubar and Hartmann 2008; Potter and Cess 2004; Wang and Rossow 1998; Weare 2000; Yan et al. 2016). This study focuses on statistically analysing the vertical distribution of clouds over the Udaipur region. In this study, we present a statistical analysis of CBH during 2021-22 using ground-based observations from the Ceilometer Lidar stationed in Udaipur. CTH properties from MODIS are used to quantify the occurrence of various cloud types. This study also evaluates the performance of reanalysis and satellite-derived CBH over the study region. Udaipur's unique geographical location, surrounded by lakes and mountains, and its climate characterized by hot and dry conditions with limited rainfall, makes it an interesting site for studying cloud behavior. The presence of surface water bodies and orographic features enhances the potential for cloud formation and provides a natural laboratory for investigating how these elements interact with atmospheric conditions to produce clouds. By analyzing CBHs using a combination of ground-based and satellite-derived data, we provide insights into the characteristics of clouds over the Udaipur region which will be potentially useful for the development of predictive models for similar environments. The rest of the paper is outlined as follows. Section 2 describes the various data sources used in this study. The key findings are presented in Sect. 3 as results and discussions. Finally, the study is concluded in Sect. 4 with a summary.

2 Study region

Udaipur, an urban city located in the desert land of the Aravalli ranges of Western India, is surrounded by lakes and mountains. The climate of Udaipur is usually hot and dry, with scanty rainfall occurring primarily during the wet season. Known as the city of lakes and a renowned tourist spot in India, Udaipur's surface water bodies and orographic features play essential roles in cloud formation. This study investigates cloud base height over the Udaipur region using ground-based Lidar (Ceilometer), satellite (MODIS), and reanalysis (ERA5) datasets. The measurement site's location and the Ceilometer Lidar installed at the roof top of Udaipur Solar Observatory's main office are shown in Fig. 1.

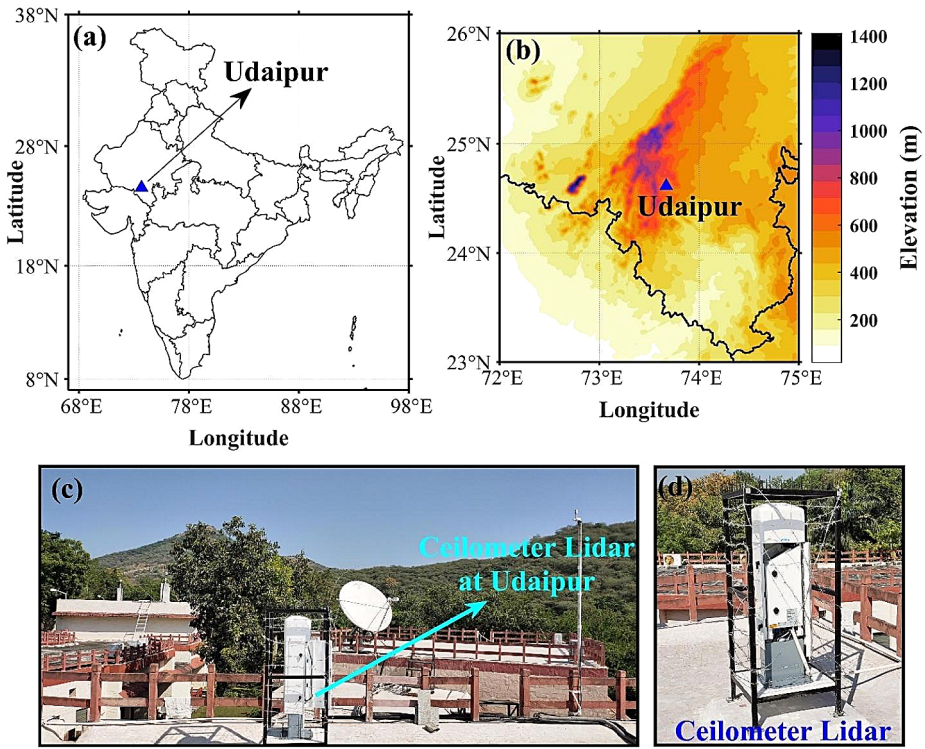


Fig. 1 (a) Location of Udaipur on the map of India, (b) elevation (in meters) map of Udaipur region using 30 s United States Geological Survey (USGS) data, (c) Ceilometer Lidar installed at the rooftop of Udaipur Solar Observatory (USO), main office at Udaipur, and (d) Ceilometer Lidar instrument

3 Data

3.1 Ceilometer Lidar (CL31)

The Ceilometer (CL31) used in this study is a low-power, pulsed Lidar instrument used to detect cloud base heights at up to three different layers simultaneously. It employs an Indium Gallium Arsenide (InGaAs) diode laser with a central wavelength of 910 nm (at 25 °C) and operates at a repetition rate of 10 kHz, enabling atmospheric sounding up to approximately 7.6 km (Martucci et al. 2010). The pulse width of the laser is around 110 ns, with an average power output of 12 mW. The backscattered light from atmospheric components such as aerosols, water vapor, and clouds is detected by a silicon avalanche photodiode. The instrument identifies cloud base heights from the extinction profile through which single and multi-layer clouds is derived. Additionally, it provides data on vertical visibility and the altitude of the highest detected signal when the sky is fully obscured due to haze, fog, and during rain. In this study, the Ceilometer data are utilized with a vertical resolution of 10 m and 16 s temporal resolution to study the cloud characteristics over the Udaipur region.

3.2 MODIS

The Moderate Resolution Imaging Spectroradiometer (MODIS) is among the five instruments aboard the Terra and Aqua satellites, which were launched in December 1999 and May 2002, respectively. These satellites, operating in a near-polar sun-synchronous orbit at an altitude of approximately 705 km, provide extensive land, ocean, and atmospheric data (Platnick et al. 2003). Terra observes the Earth during its descending node at 10:30 am, while Aqua does so during its ascending node at 1:30 pm. MODIS captures data across 36 spectral bands ranging from 0.4 μm to 14.38 μm , facilitating comprehensive studies of terrestrial, oceanic, and atmospheric phenomena. Further information about MODIS can be found at <https://modis.gsfc.nasa.gov/>. This study utilizes the MODIS/Aqua Level-2 cloud properties dataset (L2 5 Min Swath 1 km) to examine cloud characteristics over the Udaipur region.

3.3 ERA5 reanalysis

The European Centre for Medium-Range Weather Forecasts (ECMWF) generates comprehensive datasets for land surfaces, oceans, and the atmosphere, serving both research and commercial purposes through climate reanalysis. The latest iteration in this series, ERA5, represents the fifth generation of ECMWF reanalysis, produced by the Copernicus Climate Change Service (Hersbach et al. 2020). ERA5 reanalysis products integrate model data with observational data to create a consistent and comprehensive global dataset. These datasets are freely accessible and can be downloaded from the Climate Data Store (CDS, <https://cds.climate.copernicus.eu>). This study employs ERA5 hourly cloud base height data, provided at a spatial resolution of $0.25^\circ \times 0.25^\circ$ ($\sim 27 \text{ km} \times 27 \text{ km}$), for the Udaipur region.

4 Results and discussions

4.1 Cloud occurrence and cloud layer statistics over Udaipur

This section utilizes data obtained from Ceilometer Lidar to analyse the cloud occurrence and cloud layers over the Udaipur region during 2021–2022. Data was available for about 75% of the study period. However, in April 2022, there was a complete absence of data due to Ceilometer maintenance. The Ceilometer measures the atmospheric backscatter every 16 s to categorize cloud status into single and multilayer clouds, including no cloud situations and a full obscuration, which occurs when the sky/cloud is obstructed by haze, fog, dust, smoke, or rain. Fig. 2 shows the monthly frequency of different cloud layers (1, 2, and 3) and full obscuration. The occurrence frequency of a cloud layer is calculated as the ratio of the number of observations when that layer is present to the total number of observations. Total detection refers to instances when either clouds or full obscuration were present. The total detection during the observation period was about 31%, with cloud frequency (occurrence of at least one cloud layer) about 27% and full obscuration (haze, fog, and rain) $\sim 4\%$. Out of the total cloud frequency, single layer, double layer, and triple layer clouds occurred about 26.3%, 0.61%, and 0.006%, respectively. The annual cloud frequency ($\sim 27\%$) over the Udaipur region is significantly lower compared to the urban location of Ahmedabad

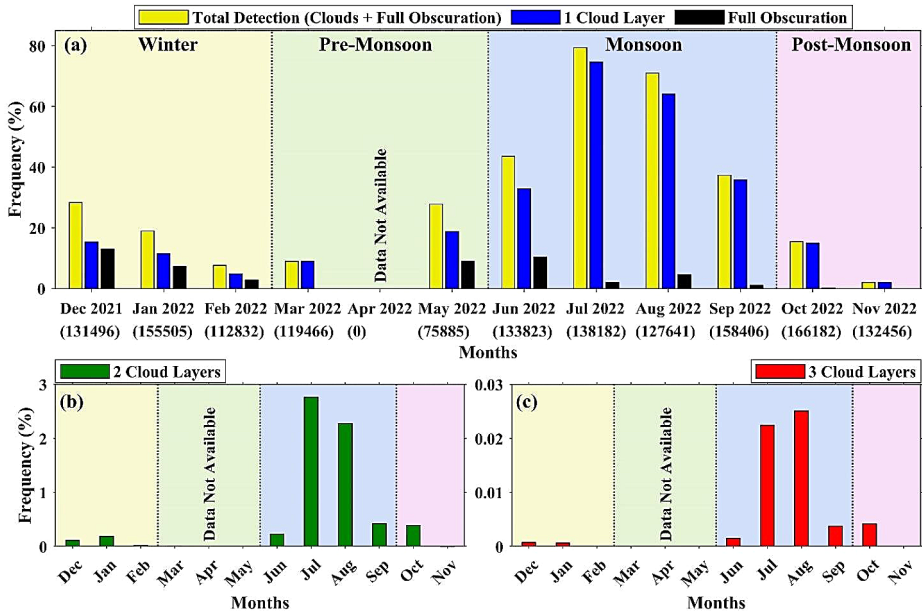


Fig. 2 (a) Monthly total detection (clouds+full obscuration), frequency of single layer clouds, and full obscuration (fog, haze, rain, etc.) over Udaipur during 2021–2022. The number in brackets below the month's name is showing the total number of observations from the Ceilometer. (b) Frequency of two-layer clouds. (c) Frequency of three-layer clouds

(23.03°N, 72.54°E) in the Western-Indian region. Vaishnav et al. (2019) has found annual cloud frequency of ~ 64% over the Ahmedabad region during 2014–2015. This suggests the less availability of moisture over the Udaipur region for the cloud formation. Due to the prevalent clear sky conditions, the study site is part of the Global Oscillation Network Group (GONG), which includes ground-based stations dedicated to helioseismology (Hill 2018).

Fig. 2a depicts the monthly frequency of single-layer clouds and full obscuration. Single-layer clouds were observed throughout the year and constituted the majority of cloud occurrences. They were particularly dominant in March and November. The highest frequency of single-layer clouds occurred during the monsoon season, with frequencies of approximately 33%, 75%, 64%, and 36% in June, July, August, and September, respectively. Full obscuration was most prevalent during the winter, peaking at about 13% in December, mainly due to fog. This fog is prevalent in Udaipur because of the presence of surface water bodies, which play a crucial role in fog formation by providing moisture (Hůnová et al. 2022). The study site is near Fateh Sagar Lake, an artificial lake with an area of around 4 km². During the monsoon season, obscuration mainly occurs due to rain, with full obscuration frequencies of 10%, 2%, 4.6%, and 1.1% in June, July, August, and September, respectively. Total cloud or full obscuration detection is low in February and March, at about 8% and 9%, respectively. November has mostly clear skies, with the lowest detection of clouds or obscured sky at around 2%.

Multi-layer clouds are more prevalent during the monsoon. Two cloud layers were most common in July and August, with frequencies of approximately 2.7% and 2.2%, respec-

tively (Fig. 2b). Similarly, three cloud layers were predominantly observed during these months, with frequencies around 0.022% and 0.025%, respectively (Fig. 2c). Notably, the third layer of clouds was absent during February, March, May, and November. The occurrence of multi-layer clouds in Udaipur was found to be lower compared to other tropical stations in India. In a study, conducted by Narendra Reddy et al. (2018) over Gadanki (13.45° N, 79.16° E), India it was observed that multi-layer clouds persist across all seasons, with the highest occurrence during the monsoon. Vaishnav et al. (2019) reported a peak occurrence of double-layer clouds during the pre- and post-monsoon periods and triple-layer clouds during the monsoon over a semi-arid region of Ahmedabad, India.

4.2 Cloud base height (CBH) characteristics over Udaipur

CBH is a fundamental characteristic of clouds, influencing the balance of shortwave radiation reaching the Earth's surface and longwave radiation emitted from the surface into space. The presence of thick low clouds typically cools the atmosphere by reducing incoming shortwave radiation and enhancing outgoing longwave radiation compared to clear sky conditions (Lee et al. 2001). Conversely, thin high clouds tend to warm the atmosphere by amplifying downward shortwave radiation and diminishing upward longwave radiation (Slingo and Slingo 1988). Therefore, the changes in CBH affect the radiation budget and significantly affect the climate system. The Ceilometer Lidar used in this study can detect up to three layers of clouds, provided that the emitted laser signal is not completely attenuated by the lowest cloud layer. The cloud base heights for the first, second, and third layers from the bottom are referred to as CBH1, CBH2, and CBH3, respectively. Fig. 3 presents

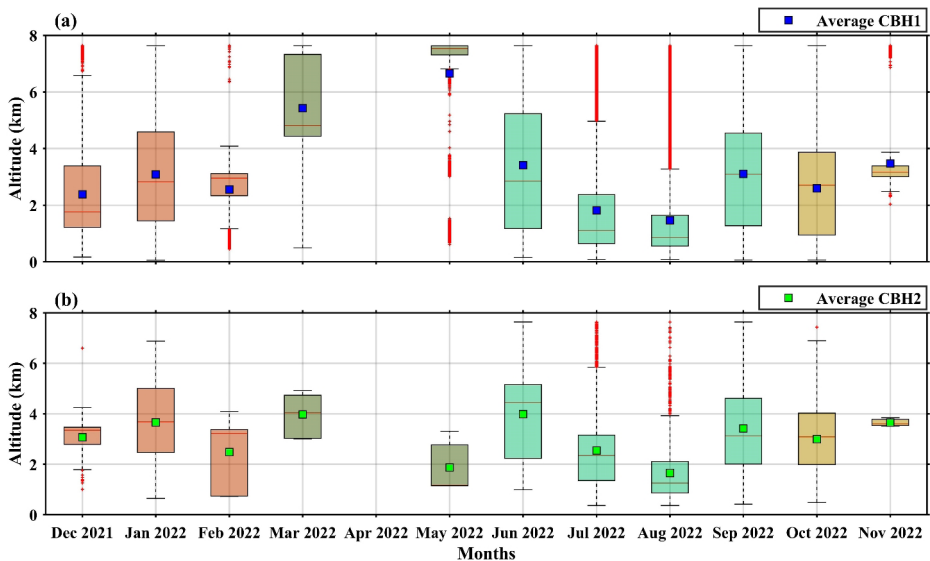


Fig. 3 Box plot showing (a) CBH1 and (b) CBH2 observed over Udaipur using Ceilometer during 2021–2022. The blue and green squares in each box represents the average value, the central line is median, edges indicate the 25th and 75th percentiles values, and red '+' symbol are outliers. Whiskers are drawn with 1.5 times of the Inter Quartile Range (IQR)

the monthly statistics of CBH1 and CBH2 over the Udaipur region for the years 2021–2022. CBH3 is not included due to the limited number of occurrences.

During the monsoon season, the average CBH1 remains below 4 km, reaching a minimum in August. Specifically, the average CBH1 values are 3.4 km, 1.8 km, 1.4 km, and 3.1 km in June, July, August, and September, respectively (Fig. 3a). Conversely, CBH1 exceeds 5 km in March and May, indicating a prevalence of high-level clouds during these months. Outliers in CBH1 are most prominent in May, July, and August, while they are absent in January, March, June, September, and October. Notably, the Inter-Quartile Range (IQR) exhibits substantial monthly variations, ranging from approximately 4 km in June to 0.5 km in May. Figure 3b illustrates that the average CBH2 mirrors the pattern observed for average CBH1 across most months. Notably, the IQR for CBH2 generally appears smaller compared to CBH1 throughout the year. Outliers in CBH2 occur exclusively in December, July, August, and October.

Figure 4 (a, b, c) shows the probability density of various cloud layers (CBH1, CBH2, and CBH3) over Udaipur across different height ranges. The height range from 0 to 8 km is divided into eight 1 km bins. As the third cloud layer is not observed above 7 km, it has only seven bins. The CBH1 is most frequently observed below 1 km, while CBH2 and CBH3 are most commonly found between 1 and 2 km. Above 1 km, CBH2 shows a continuous decline in probability density with height, whereas CBH3 is mainly concentrated between 1 and 4 km. Fig. 4d shows the diurnal variation of cloud frequency over Udaipur for the period 2021–2022. The frequency distribution was calculated for different hours of the day. The frequency of total cloud detection and the first cloud layer remains steady at around 4% throughout both day and night. This indicates that cloud occurrence is evenly distributed over the 24-hour period. The second layer frequency exceeds 4% from 10:00 PM to 05:00 AM local time, indicating a higher occurrence during nighttime. The frequency of third

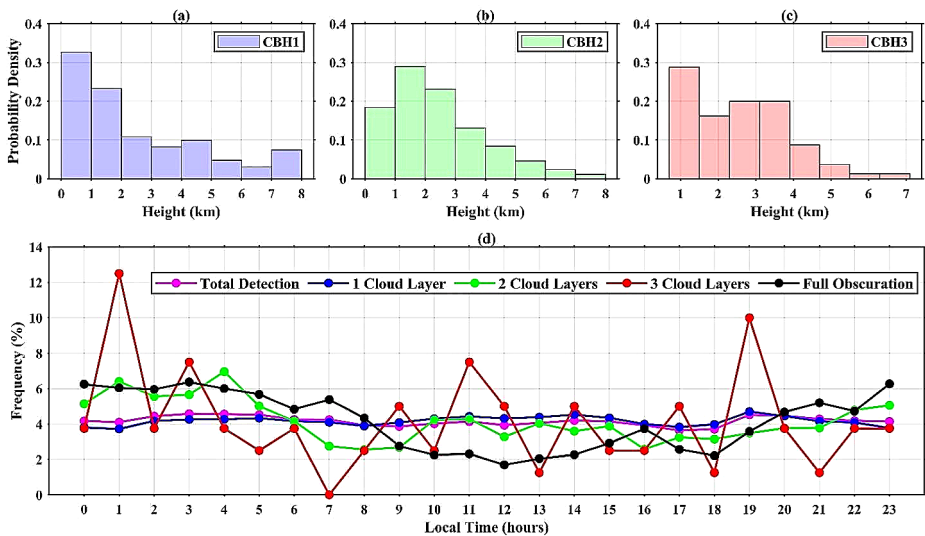


Fig. 4 (a, b & c) Probability density of cloud layers CBH1, CBH2, and CBH3 in different height ranges and (d) Diurnal pattern of frequency of total detection, cloud layers (CBH1, CBH2, and CBH3), and full obscuration.

layer clouds peaks between 01:00–02:00 AM, 11:00 AM–12:00 PM, and 7:00–8:00 PM. Notably, sky obscuration is greater during nighttime than daytime.

4.3 Cloud observation over Udaipur using MODIS

A total of 735 sample observations by MODIS were analysed to study the cloud top properties over the Udaipur region during the study period (2021–2022). Out of the total MODIS passes over Udaipur, CTH was reported 270 times. Fig. 5a illustrates the CTH observed from MODIS over Udaipur, showing that most clouds were observed during the monsoon season. The observed CTH ranged from approximately 0.2 km to 16 km, with 14% occurring between 0 and 2 km, 25% between 2 and 6 km, and 61% above 6 km.

Of the 270 cloud observations, cloud top pressure and cloud optical thickness data were available for 102 instances. These parameters were used to classify clouds into various types according to the International Satellite Cloud Climatology Project (ISCCP) cloud classification (Rossow et al., 1999). The clouds observed by MODIS were categorized into nine types: cumulus, stratocumulus, stratus (low clouds), altocumulus, altostratus, nimbostratus (mid clouds), and cirrus, cirrostratus, cumulonimbus (high clouds). Cirrostratus clouds were the most frequent, occurring 36% of the time, while stratus (<1%) and altocumulus (2%) clouds were the least common (Fig. 5b). The occurrences of cumulonimbus, altostratus, and cirrus clouds were 13%, 17%, and 10%, respectively.

The cloud top properties from MODIS are used to derive the CBH. The CBH is derived using the CTH and cloud geometrical thickness (CGT), where CGT depends on the micro-physical properties of the cloud (Seaman et al. 2017).

$$CBH = CTH - CGT \tag{1}$$

For liquid clouds,

$$CGT = \frac{LWP}{LWC} \tag{2}$$

where, LWP (liquid water path) depends on cloud optical thickness and cloud effective radius (Liou 1992), and the value of LWC (liquid water content) varies with the cloud type.

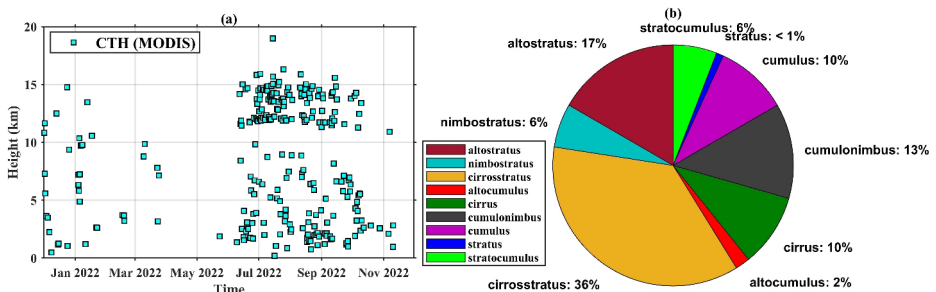


Fig. 5 (a) Cloud Top Height (CTH) observed by MODIS over the Udaipur region during the study period (b) Percentage of occurrence of different cloud types (classification as per ISCCP on the basis of cloud top temperature and cloud optical thickness).

In this study, MODIS/Aqua Level-2 cloud properties product available at 1 km spatial resolution is utilized to derive the CBH. To calculate the CBH, first clouds are classified using the ISCCP cloud classification based on cloud top pressure and cloud optical thickness. The LWC for each cloud type as specified by ISCCP is applied to calculate the CGT using Eq. 2, and subsequently CBH is derived using Eq. 1. However, there are some limitations in deriving CBH from MODIS data. First, CBH can only be derived from MODIS during the daytime because cloud optical thickness and cloud effective radius are obtained from sunlight reflectance off clouds. Another limitation of the algorithm is the assumption that LWC is constant throughout the geometrical thickness of the cloud (Hutchison 2002). For comparison purposes, the nearest MODIS pixel from the Ceilometer site is utilized throughout the study.

Out of 102 cloud detections, 51 instances were identified as liquid phase clouds. For these water clouds, CBH was calculated using Eqs. 1 and 2. Table 1 presents a comparison between ground-based Ceilometer observation of clouds (CBH1 and CBH2) and the

Table 1 Comparison between Ceilometer Cloud base height (CBH1 & CBH2) and MODIS derived CBH for liquid phase clouds over Udaipur during December 2021 to November 2022

S.no.	Date/Time (UTC)	MODIS CTH (km)	MODIS CBH (km)	Ceilometer CBH1 (km)	Ceilometer CBH2 (km)
1	2021-12-03 07:20	3.628	3.478	2.027	NaN
2	2022-01-04 09:00	5.811	5.443	4.305	4.705
3	2022-01-05 08:05	4.882	4.715	3.408	NaN
4	2022-03-23 09:10	3.176	3.116	NaN	NaN
5	2022-06-14 07:50	2.521	2.243	1.949	2.235
6	2022-06-16 09:15	1.546	1.459	1.582	NaN
7	2022-06-18 09:05	2.298	2.245	1.982	2.46
8	2022-06-19 08:05	3.081	2.888	1.599	NaN
9	2022-06-26 08:10	5.524	5.348	3.077	3.095
10	2022-06-28 08:00	3.894	3.47	1.36	NaN
11	2022-07-04 09:00	6.369	6.013	4.054	NaN
12	2022-07-12 08:10	5.238	4.658	1.217	2.025
13	2022-07-22 08:45	3.793	3.337	2.221	2.215
14	2022-07-31 08:35	2.912	1.209	0.976	NaN
15	2022-08-17 07:35	1.389	1.338	0.71	NaN
16	2022-08-18 08:20	2.032	1.672	0.987	NaN
17	2022-08-19 09:00	3.866	3.766	1.616	1.715
18	2022-08-24 07:40	5.877	5.477	0.406	0.665
19	2022-08-26 07:30	3.724	3.557	1.022	1.155
20	2022-09-09 09:15	1.881	1.744	2.917	NaN
21	2022-09-11 07:25	1.68	1.593	3.964	3.705
22	2022-09-12 08:05	3.666	3.198	1.108	NaN
23	2022-09-15 08:35	6.628	6.304	4.615	NaN
24	2022-09-25 07:35	1.174	1.084	1.173	NaN
25	2022-09-25 09:10	1.288	1.268	NaN	NaN
26	2022-10-04 07:25	4.296	4.064	2.547	NaN
27	2022-10-06 08:50	4.065	3.945	4.368	NaN
28	2022-10-07 07:55	5.42	5.02	2.291	NaN
29	2022-10-08 08:35	5.58	4.82	0.974	1.815
30	2022-10-09 07:40	2.366	2.219	2.12	2.175

MODIS-derived CTH and CBH for liquid phase clouds. Notably, the Ceilometer did not observe a third cloud layer during any MODIS passes over Udaipur in this study. A comparison of MODIS-derived CBH and Ceilometer observations on 14 June 2022, 16 June 2022, 31 July 2022, and 9 September 2022 is depicted in Fig. 6. On 31 July 2022, MODIS retrieved a CTH of 2.9 km and a derived CBH of 1.2 km, which is approximately 100 m higher than the Ceilometer’s observed CBH. Fig. 6b shows that CTH from MODIS is slightly lower than the Ceilometer-observed clouds. This discrepancy could be due to the spatial differences between the MODIS and ground-based observations. Numerous studies have compared the CTH and CBH derived from MODIS with ground-based observations across various regions to estimate the bias (Baum et al. 2012; Huo et al. 2020; Kim et al. 2011; Sharma et al. 2016; Sporre et al. 2016). Huo et al. (2020) found that CTH from MODIS above 6 km shows lesser discrepancies compared to those below 4 km. Sporre et al. (2016) investigated CTH from MODIS and found that satellites overestimated CTH for single-layer clouds but underestimated it for multilayer clouds. Comparing and validating satellite-derived cloud properties with ground-based observations is crucial for improving the techniques used for cloud product retrieval.

Figure 7 compares MODIS-derived cloud top and base heights for liquid and ice phase clouds with Ceilometer observations. This study is limited to deriving cloud base height from MODIS only for liquid-phase clouds. The CTH retrieved by MODIS for ice phase clouds (Fig. 7a, b, and c) is above 8 km, beyond the Ceilometer’s range. However, for these cases Ceilometer reported cloud bases below 4 km, indicating the presence of multilayer clouds. For liquid phase clouds on June 23, July 19, and July 22, the cloud base height

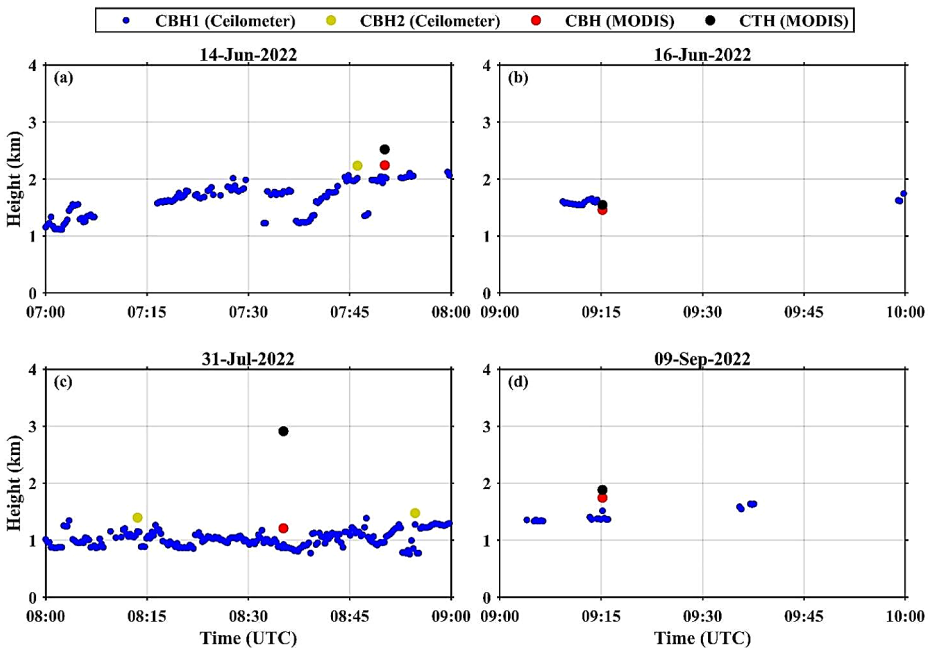


Fig. 6 MODIS derived Cloud Top Height (CTH) and Cloud Base Height (CBH) for low-level clouds compared with the Ceilometer observed CBH over the Udaipur region. The CBH derived from the MODIS closely match the observations from the Ceilometer

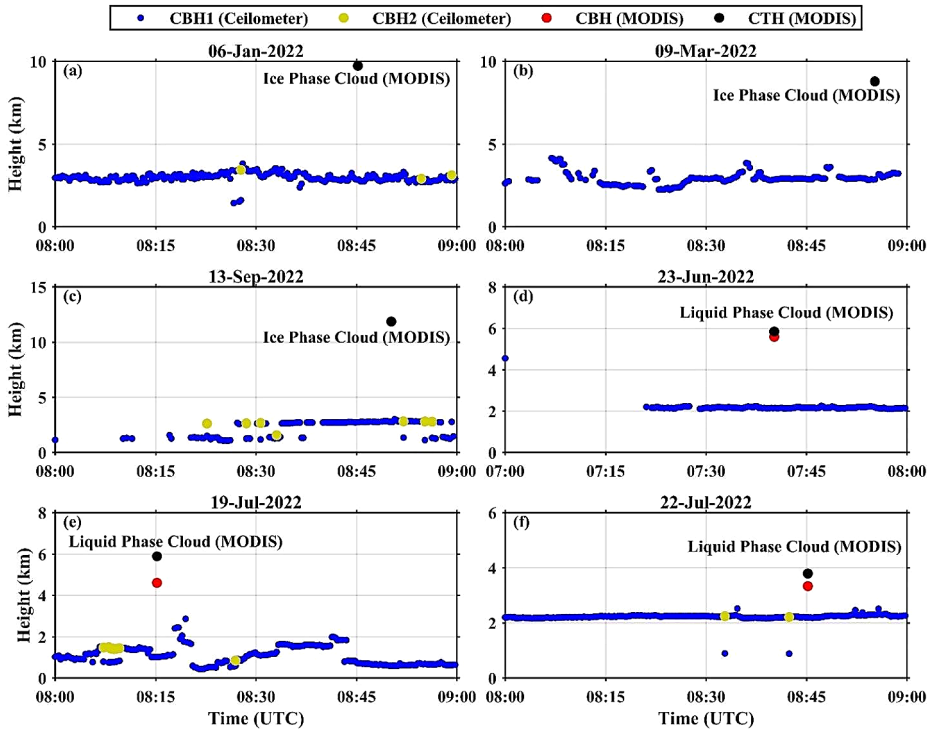


Fig. 7 Comparison of MODIS derived Cloud Top Height (CTH) and Cloud Base Height (CBH) for ice phase clouds (a, b, c) and liquid phase clouds (d, e, f) with the Ceilometer observed CBH1 and CBH2

derived using MODIS differed from Ceilometer CBH by approximately 3.7 km, 3.6 km, and 1.1 km, respectively. It is noteworthy that for low-level clouds below 2 km, the cloud base height derived using MODIS closely matches ground observations (Fig. 6). However, for clouds above 2 km, the discrepancy between the two CBH measurements is larger, indicating that the algorithm performs better for low-level thick clouds.

4.4 Comparison of CBH derived from ERA5 with the Ceilometer

The ERA5 reanalysis provides CBH data with an hourly temporal resolution. For multilayer clouds, it only reports the base height of the lowest cloud layer. The CBH in ERA5 is determined as the lowest altitude where the cloud fraction exceeds 1% and the condensate content surpasses 10^{-6} kg/kg, starting from the second-lowest level upwards (Hersbach et al. 2020). This study assesses the performance of ERA5 in estimating CBH over the Udaipur region by comparing it with observations from a Ceilometer. Given the Ceilometer's vertical range is limited to approximately 7.6 km, the analysis is confined to cloud observations below this altitude.

In a dataset comprising 3,236 instances of hourly cloud observations from both the Ceilometer and ERA5, the Ceilometer detected clouds 2,844 times, while ERA5 detected clouds 2,704 times. Table 2 presents a detailed comparison of cloud detection between the Ceilometer and ERA5. The detection efficiency of ERA5, defined as the percentage of cases

Table 2 Table showing the cloud representation by Ceilometer and ERA5 over Udaipur during December 2021 to November 2022

S.no.	Ceilometer	ERA5	Percentage
1	Cloud detected (Yes)	Cloud detected (No)	11.46%
2	Cloud detected (Yes)	Cloud detected (Yes)	76.42%
3	Cloud detected (No)	Cloud detected (Yes)	7.14%
4	Cloud detected (No)	Cloud detected (No)	4.98%

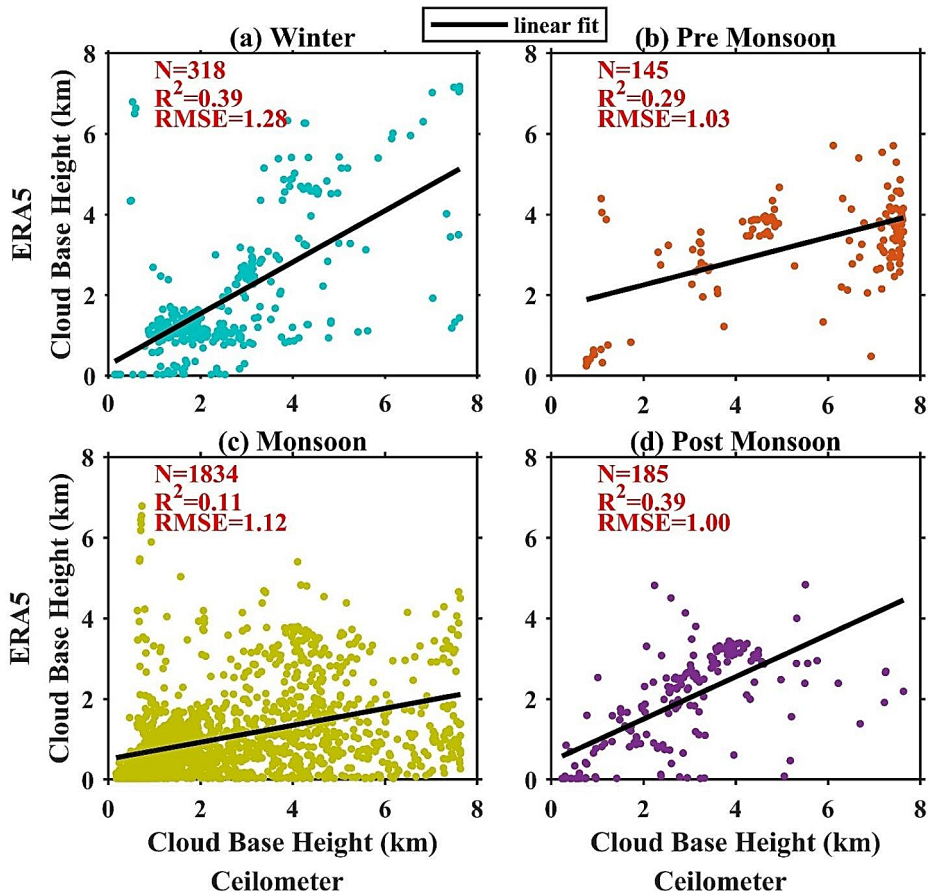


Fig. 8 Comparison of ERA5 hourly cloud base height data with the Ceilometer observed hourly average CBH in different seasons

where ERA5 detected clouds also observed by the Ceilometer, is approximately 76.42%. Conversely, in 11.46% of the cases, ERA5 failed to estimate the clouds that were observed by the Ceilometer.

The seasonal correlation between ERA5 and Ceilometer cloud base heights is illustrated in Fig. 8. During winter (December, January, February), there are 318 instances where both ERA5 and the Ceilometer detected clouds below 7.6 km, with a correlation coefficient (R^2) of 0.39 and a root mean square error (RMSE) of approximately 1.28 km. For the pre-monsoon period (March, April, May), the ERA5 shows a correlation of 0.29 with the Ceilometer,

with an RMSE of around 1.03 km. The highest frequency of cloud observations occurs during the monsoon season (June, July, August, September), with 1834 cases of mutual detection below 7.6 km, but the correlation is the lowest (0.11) with an RMSE of 1.12 km. In the post-monsoon period, the correlation improves, with R^2 and RMSE values of 0.39 and 1 km, respectively. The ERA5 reanalysis tends to underestimate mid-level and high-level clouds during the monsoon season. Discrepancies in the ERA5 cloud parameters may result from the parameterization schemes used in the reanalysis model and differences in spatial resolution. The discrepancies in the ERA5 cloud parameters have been previously reported in several studies (Kundu et al. 2023; Wang et al. 2022; Yao et al. 2020a). These discrepancies arise due to lack of observations assimilated in the assimilation models. Due to the limitations of assimilation models, incorporating cloud observations into reanalysis is challenging, and cloud properties are largely parameterized (Yao et al. 2020b). Biases in these cloud properties lead to uncertainties in weather and climate models (Wu et al. 2024). Therefore, evaluating and improving reanalysis products is crucial for atmospheric research.

5 Summary and conclusions

The investigation of cloud base height (CBH) over Udaipur, an urban city in the Aravalli ranges of Western India, has been conducted for the first-time using ground-based Lidar, satellite, and reanalysis datasets. The study reveals that clouds predominantly appear during the monsoon season, with the highest frequency in July. While cloud occurrence is similar during both day and night, full sky obscuration is primarily a nighttime phenomenon caused by fog, which forms from the interaction of cool air with warm, moist air over the city's surrounding lakes. The research shows that the average CBH is lower during the monsoon and higher in the pre-monsoon and post-monsoon periods. Comparisons indicate that MODIS satellite-derived cloud base heights align with Ceilometer observations for low clouds but not for high clouds. Further, cirrostratus clouds are identified as the most common type, accounting for about 36% of cloud observations; despite alignment, the correlation between MODIS derived CBH and Ceilometer observations is generally weak. This discrepancy underscores the necessity of regular ground-based observations of clouds. Additionally, the ERA5 reanalysis data fail to accurately estimate the CBH, exhibiting low correlation with the Ceilometer observations. Therefore, ground-based Ceilometer observations are crucial for validating and refining regional weather and climate models by filling in data gaps that lead to model discrepancies. In the future, continuous cloud observations using Ceilometers will be vital for assessing the impact of clouds on the radiation budget in this region, enhancing our understanding and prediction of local weather and climate dynamics.

Acknowledgements The authors are thankful to NASA for MODIS satellite products freely available at <https://ladsweb.modaps.eosdis.nasa.gov/>. Authors are also thankful to the ECMWF for providing ERA5 cloud base height data, freely available at <https://cds.climate.copernicus.eu/>. We are grateful to the Director, PRL for helping in setting up the Lidar laboratory at Udaipur station under PRL's ILIN (Indian Lidar Network) program. We are thankful to Dr. Brajesh Kumar for his help in regular operation of the Ceilometer Lidar at Udaipur Solar Observatory (USO), Udaipur. We would also like to thank Prof. (Mrs.) Nandita Srivastava, Prof. Shibu K Mathew, and other staff members at USO, for their help and support. The authors are thankful to the Indian Space Research Organization Geosphere Biosphere Program (ISRO-GBP) of the Department of Space, Government of India for support. This work is supported by the Physical Research Laboratory, Department of Space, Government of India.

Author contributions D.K.K. - conceptualization, data analysis, writing first draft, revision. S.K.K. - supervision, investigation, corrections and editing, revision. N.K.K. - discussions, suggestions, corrections and editing. P.K. - investigations, software, corrections and editing, revision. S.S. - discussions and constructive suggestions.

Funding The authors declare that no funds, grants, or other support were received during the preparation of this manuscript. The authors have no relevant financial or non-financial interests to disclose.

Data availability The datasets used in this study are freely available and can be downloaded from the following: ERA5 Reanalysis: <https://cds.climate.copernicus.eu/> MODIS Satellite cloud properties products: <https://ladsweb.modaps.eosdis.nasa.gov/>. Ceilometer data will be made available on reasonable request.

Declarations

Competing interests The authors declare no competing interests.

References

- An N, Pinker R, Wang K, E.R.-I.J. of (2020) undefined, 2019. Evaluation of cloud base height in the North American Regional Reanalysis using ceilometer observations. *Wiley Online Library* 40, 3161–3178. <https://doi.org/10.1002/joc.6389>
- Baum BA, Menzel WP, Frey RA, Tobin DC, Holz RE, Ackerman SA, Heidinger AK, Yang P (2012) MODIS Cloud-Top Property Refinements for Collection 6. <https://doi.org/10.1175/JAMC-D-11-0203.1>
- Bony S, Colman R, Kattsov VM, Allan RP, Bretherton CS, Dufresne JL, Hall A, Hallegatte S, Holland MM, Ingram W, Randall DA, Soden BJ, Tselioudis G, Webb MJ (2006) How well do we understand and evaluate climate change feedback processes? *J Clim* 19:3445–3482. <https://doi.org/10.1175/JCLI3819.1>
- Cess RD, Potter GL, Blanchet JP, Boer GJ, Ghan SJ, Kiehl JT, Le Treut H, Li ZX, Liang XZ, Mitchell JFB, Morcrette JJ, Randall DA, Riches MR, Roeckner E, Schlese U, Slingo A, Taylor KE, Washington WM, Wetherald RT, Yagai I (1989) Interpretation of cloud-climate feedback as produced by 14 atmospheric general circulation models. *Science* 245:513–516. <https://doi.org/10.1126/SCIENCE.245.4917.513>
- Costa-Surós M, Calbó J, González JA, Martín-Vide J (2013) Behavior of cloud base height from ceilometer measurements. *Atmos Res* 127:64–76. <https://doi.org/10.1016/J.ATMOSRES.2013.02.005>
- Hersbach H, Bell B, Berrisford P, Hirahara S, Horányi A, Muñoz-Sabater J, Nicolas J, Peubey C, Radu R, Schepers D, Simmons A, Soci C, Abdalla S, Abellan X, Balsamo G, Bechtold P, Biavati G, Bidlot J, Bonavita M, De Chiara G, Dahlgren P, Dee D, Diamantakis M, Dragani R, Flemming J, Forbes R, Fuentes M, Geer A, Haimberger L, Healy S, Hogan RJ, Hólm E, Janisková M, Keeley S, Laloyaux P, Lopez P, Lupu C, Radnoti G, de Rosnay P, Rozum I, Vamborg F, Villaume S, Thépaut JN (2020) The ERA5 global reanalysis. *Q J R Meteorol Soc* 146:1999–2049. <https://doi.org/10.1002/QJ.3803>
- Hill F (2018) The Global Oscillation Network Group Facility—An example of Research to operations in Space Weather. *Space Weather* 16:1488–1497. <https://doi.org/10.1029/2018SW002001>
- Hůnová I, Brabec M, Geletič J, Malý M, Dumitrescu A (2022) Local fresh- and sea-water effects on fog occurrence. *Sci Total Environ* 807:150799. <https://doi.org/10.1016/j.scitotenv.2021.150799>
- Huo J, Li J, Duan M, Lv D, Han C, Bi Y (2020) Measurement of Cloud Top Height: comparison of MODIS and Ground-based Millimeter Radar. *Remote Sens* 12:1616. <https://doi.org/10.3390/rs12101616>
- Hutchison KD (2002) The retrieval of cloud base heights from MODIS and three-dimensional cloud fields from NASA's EOS Aqua mission. *Int J Remote Sens* 23:5249–5265. <https://doi.org/10.1080/01431160110117391>
- Kim S-W, Chung E-S, Yoon S-C, Sohn B-J, Sugimoto N (2011) Intercomparisons of cloud-top and cloud-base heights from ground-based Lidar, CloudSat and CALIPSO measurements. *Int J Remote Sens* 32:1179–1197. <https://doi.org/10.1080/01431160903527439>
- King MD, Platnick S, Menzel WP, Ackerman SA, Hubanks PA (2013) Spatial and temporal distribution of clouds observed by MODIS Onboard the Terra and Aqua satellites. *IEEE Trans Geosci Remote Sens* 51:3826–3852. <https://doi.org/10.1109/TGRS.2012.2227333>
- Kubar TL, Hartmann DL (2008) Vertical structure of tropical oceanic convective clouds and its relation to precipitation. *Geophys Res Lett* 35:3804. <https://doi.org/10.1029/2007GL032811>

- Kundu A, Kundu SS, Sharma SK, Gogoi M, Banik T, Borgohain A, Mahanta R, Debnath A (2023) The behavior of cloud base height over a hilly remote station of North-East India using ground-based remote sensing technique. *Atmos Res* 282:106512. <https://doi.org/10.1016/j.atmosres.2022.106512>
- Lee M-I, Kang I-S, Kim J-K, Mapes BE (2001) Influence of cloud-radiation interaction on simulating tropical intraseasonal oscillation with an atmospheric general circulation model. *J Geophys Res: Atmos* 106:14219–14233. <https://doi.org/10.1029/2001JD900143>
- Lee S, Hwang SO, Kim J, Ahn MH (2018) Characteristics of cloud occurrence using ceilometer measurements and its relationship to precipitation over Seoul. *Atmos Res* 201:46–57. <https://doi.org/10.1016/J.ATMOSRES.2017.10.010>
- Liou K (1992) Radiation and cloud processes in the atmosphere. Theory, observation, and modeling
- Lü Q, Li J, Wang T, Huang J (2015) Cloud radiative forcing induced by layered clouds and associated impact on the atmospheric heating rate. *J Meteorological Res* 29:779–792. <https://doi.org/10.1007/S13351-015-5078-7/METRICS>
- Martucci G, Milroy C, O'Dowd CD (2010) Detection of cloud-base height using Jenoptik CHM15K and Vaisala CL31 Ceilometers. *J Atmos Ocean Technol* 27:305–318. <https://doi.org/10.1175/2009JTECHA1326.1>
- Maturilli M, Ebell K (2018) Twenty-five years of cloud base height measurements by ceilometer in Ny-Ålesund. *Svalbard Earth Syst Sci Data* 10:1451–1456. <https://doi.org/10.5194/ESSD-10-1451-2018>
- Narendra Reddy N, Venkat Ratnam M, Basha G, Ravikiran V (2018) Cloud vertical structure over a tropical station obtained using long-term high-resolution radiosonde measurements. *Atmos Chem Phys* 18:11709–11727. <https://doi.org/10.5194/acp-18-11709-2018>
- Platnick S, King MD, Ackerman SA, Menzel WP, Baum BA, Riédi JC, Frey RA (2003) The MODIS cloud products: algorithms and examples from terra. *IEEE Trans Geosci Remote Sens* 41:459–472. <https://doi.org/10.1109/TGRS.2002.808301>
- Potter GL, Cess RD (2004) Testing the impact of clouds on the radiation budgets of 19 atmospheric general circulation models. *J Geophys Res: Atmos* 109:2106. <https://doi.org/10.1029/2003JD004018>
- Ramanathan V, Cess RD, Harrison EF, Minnis P, Barkstrom BR, Ahmad E, Hartmann D (1989) Cloud-radiative forcing and climate: results from the Earth Radiation Budget Experiment. *Science* 243:57–63. <https://doi.org/10.1126/SCIENCE.243.4887.57>
- Randall D, Khairoutdinov M, Arakawa A, Grabowski W (2003) Breaking the Cloud parameterization deadlock. *Bull Am Meteorol Soc* 84:1547–1564. <https://doi.org/10.1175/BAMS-84-11-1547>
- Samanta S, Tyagi B, Vissa NK, Sahu RK (2020) A new thermodynamic index for thunderstorm detection based on cloud base height and equivalent potential temperature. *J Atmos Solar Terr Phys* 207:105367. <https://doi.org/10.1016/J.JASTP.2020.105367>
- Schmetz J (2016) On the parameterization of the radiative properties of broken clouds. New pub: Stockholm uni Press 36 A:417–432. <https://doi.org/10.3402/TELLUSA.V36I5.11644>
- Seaman CJ, Noh Y-J, Miller SD, Heidinger AK, Lindsey DT (2017) Cloud-base height estimation from VIIRS. Part I: operational algorithm validation against CloudSat. *J Atmos Ocean Technol* 34:567–583. <https://doi.org/10.1175/JTECH-D-16-0109.1>
- Sharma S, Vaishnav R, Shukla MV, Kumar, Prashant, Kumar, Prateek, Thapliyal PK, Lal S, Acharya YB (2016) Evaluation of cloud base height measurements from Ceilometer CL31 and MODIS satellite over Ahmedabad, India. *Atmos Meas Tech* 9:711–719. <https://doi.org/10.5194/amt-9-711-2016>
- Slingo A, Slingo JM (1988) The response of a general circulation model to cloud longwave radiative forcing. I: introduction and initial experiments. *Q J R Meteorol Soc* 114:1027–1062. <https://doi.org/10.1002/QJ.49711448209>
- Sporre MK, O'Connor EJ, Håkansson N, Thoss A, Swietlicki E, Petäjä T (2016) Comparison of MODIS and VIIRS Cloud properties with ARM ground-based observations over Finland. *Atmos Meas Tech* 9:3193–3203. <https://doi.org/10.5194/amt-9-3193-2016>
- Stephens G, Webster P (1981) Clouds and climate: Sensitivity of simple systems. *journals.ametsoc.org*
- Stubenrauch CJ, Rossow WB, Kinne S, Ackerman S, Cesana G, Chepfer H, Di Girolamo L, Getzewich B, Guignard A, Heidinger A, Maddux BC, Menzel WP, Minnis P, Pearl C, Platnick S, Poulsen C, Riedi J, Sun-Mack S, Walther A, Winker D, Zeng S, Zhao G (2013) Assessment of Global Cloud datasets from satellites: Project and Database initiated by the GEWEX Radiation Panel. *Bull Am Meteorol Soc* 94:1031–1049. <https://doi.org/10.1175/BAMS-D-12-00117.1>
- Vaishnav R, Sharma S, Shukla KK, Kumar P, Lal S (2019) A comprehensive statistical study of cloud base height using ceilometer over western India. *Adv Space Res* 63:1708–1718. <https://doi.org/10.1016/J.ASR.2018.11.006>
- Viúdez-Mora A, Costa-Surós M, Calbó J, González JA (2015) Modeling atmospheric longwave radiation at the surface during overcast skies: the role of cloud base height. *J Geophys Res: Atmos* 120:199–214. <https://doi.org/10.1002/2014JD022310>

- Wang Z, Menenti M (2021) Challenges and opportunities in Lidar Remote sensing. *Front Remote Sens* 2. <https://doi.org/10.3389/FRSEN.2021.641723/FULL>
- Wang J, Rossow WB (1998) Effects of Cloud Vertical structure on Atmospheric circulation in the GISS GCM. *J Clim* 11:3010–3029
- Wang R, Zhou R, Yang S, Li R, Pu J, Liu K, Deng Y (2022) A New Algorithm for estimating low cloud-base height in Southwest China. <https://doi.org/10.1175/JAMC-D-21-0221.1>
- Weare BC (2000) Insights into the importance of cloud vertical structure in climate. *Geophys Res Lett* 27:907–910. <https://doi.org/10.1029/1999GL011214>
- Wu Y, Gao J, Zhao A (2024) Cloud properties and dynamics over the Tibetan Plateau– A review. *Earth Sci Rev* 248:104633. <https://doi.org/10.1016/j.earscirev.2023.104633>
- Xu H, Guo J, Li J, Liu L, Chen T, Guo X, Lyu Y, Wang D, Han Y, Chen Q, Zhang Y (2021) The significant role of radiosonde-measured cloud-base height in the estimation of cloud radiative forcing. *Springer* 38:1552–1565. <https://doi.org/10.1007/s00376-021-0431-5>
- Yan Y, Liu Y, Lu J (2016) Cloud vertical structure, precipitation, and cloud radiative effects over Tibetan Plateau and its neighboring regions. *J Geophys Research: Atmos* 121:5864–5877. <https://doi.org/10.1002/2015JD024591>
- Yao B, Liu C, Yin Y, Liu Z, Shi C, Iwabuchi H, Weng F (2020a) Evaluation of cloud properties from reanalyses over East Asia with a radiance-based approach. *Atmos Meas Tech* 13:1033–1049. <https://doi.org/10.5194/amt-13-1033-2020>
- Yao B, Teng S, Lai R, Xu X, Yin Y, Shi C, Liu C (2020b) Can atmospheric reanalyses (CRA and ERA5) represent cloud spatiotemporal characteristics? *Atmos Res* 244:105091. <https://doi.org/10.1016/j.atmosres.2020.105091>

Publisher's Note Springer Nature remains neutral with regard to jurisdictional claims in published maps and institutional affiliations.

Springer Nature or its licensor (e.g. a society or other partner) holds exclusive rights to this article under a publishing agreement with the author(s) or other rightsholder(s); author self-archiving of the accepted manuscript version of this article is solely governed by the terms of such publishing agreement and applicable law.

Authors and Affiliations

Dharmendra Kumar Kamat^{1,2} · Som Kumar Sharma¹ · Kondapalli Niranjan Kumar³ · Prashant Kumar⁴ · Sourita Saha⁵

✉ Som Kumar Sharma
somkumar@prl.res.in

¹ Physical Research Laboratory, Ahmedabad, India

² Indian Institute of Technology Gandhinagar, Gandhinagar, India

³ National Centre for Medium Range Weather Forecasting, Ministry of Earth Sciences, Noida, India

⁴ Space Applications Centre, Ahmedabad, India

⁵ Scripps Institution of Oceanography, University of California, San Diego, CA, USA